

# A kinetic study of the oxidation of arsenopyrite in acidic solutions: implications for the environment

Yu Yunmei<sup>a,\*</sup>, Zhu Yongxuan<sup>a</sup>, A.E. Williams-Jones<sup>b</sup>, Gao Zhenmin<sup>a</sup>,  
Li Dexian<sup>a</sup>

<sup>a</sup>*Institute of Geochemistry, Chinese Academy of Sciences, Guiyang 550002, PR China*

<sup>b</sup>*Department of Earth and Planetary Science, McGill University, Montreal, Quebec, H3A2A7 Canada*

Received 2 January 2003; accepted 31 May 2003

Editorial handling by A.H. Welch

## Abstract

Arsenopyrite is an important component of many ore deposits and dissolves in the O<sub>2</sub>-rich, acidic surface waters that are commonly found in the vicinity of active mines, releasing As, Fe and S to the environment. However, despite the potentially serious effect of this pollution on the human and animal population, the rate at which such oxidation occurs is poorly known. Kinetic experiments were therefore conducted in a mixed flow reactor to investigate the oxidation of arsenopyrite in Fe<sub>2</sub>(SO<sub>4</sub>)<sub>3</sub> solutions (pH = 1.8) having a concentration of 1 × 10<sup>-2</sup> to 1 × 10<sup>-5</sup> mol kg<sup>-1</sup> at temperatures of 45, 35, 25 and 15 °C. The results of these experiments show that the rate of oxidation of arsenopyrite increases with increasing concentration of dissolved Fe<sub>2</sub>(SO<sub>4</sub>)<sub>3</sub> and temperature. They also show that As released during the oxidation of arsenopyrite has the form As(III), and that the rate of conversion of As(III) to As(V) is relatively low, although it tends to increase with increasing concentration of dissolved Fe<sub>2</sub>(SO<sub>4</sub>)<sub>3</sub> and temperature. In the presence of Cl<sup>-</sup>, oxidation of arsenopyrite is accelerated, as is the conversion of As(III) to As(V). These findings indicate that exploitation of arsenopyrite-bearing ores will cause contamination of groundwaters by As at levels sufficient to have a major negative effect on the health of humans and animals.

© 2003 Elsevier Ltd. All rights reserved.

*Keywords:* Arsenopyrite; AMD; Mine wastes; Mine drainage; Arsenate and arsenite

## 1. Introduction

Arsenopyrite is a major component of many mineral deposits, and is the principal raw material for the industrial production of As. However, arsenopyrite also presents a serious health hazard, if major quantities of it are exposed to oxidizing waters that are subsequently used for human consumption. In such waters, arsenopyrite will decompose, releasing Fe, As, and S. Some of this solute will be adsorbed on solid phases near the site of dissolution, e.g., in a mine, but much of it will find its way into the surrounding environment and potentially into the drinking water of nearby towns and villages.

Dissolved As occurs dominantly as inorganic As(III) (arsenite) and As(V) (arsenate) ions, and if consumed in large amounts may poison the nervous and digestive systems and cause a variety of skin diseases. The acute health risk is particularly high if As(III) is dominant, as this form of dissolved As is 60 times more toxic than As(V) (Bottomley, 1984).

During the past more than 20a, a number of Carlin-type Au deposits have been found in the Yunnan–Guizhou–Guangxi golden triangle area of southwestern China, in which arsenopyrite and associated pyrite are the main ore minerals (Lixian et al., 1993). Extensive exploration and mining activity has led to widespread exposure of the sulfide minerals to the atmosphere. As a result, these sulfides are being oxidized due to interaction with O<sub>2</sub>-rich surface waters, and are decomposing,

\* Corresponding author.

E-mail address: [yum@public.gz.cn](mailto:yum@public.gz.cn) (Y. Yunmei).

acidifying the waters and enriching the waters in ions such as  $\text{SO}_4^{2-}$ ,  $\text{Cl}^-$ ,  $\text{Fe}^{3+}$ ,  $\text{Fe}^{2+}$ , and  $\text{Cu}^{2+}$ . Evidence for this is provided in Table 1, which compares the concentrations of As and anions in mine waters and spring waters from the Nanhua As–Tl and Lanmuchang Hg–As–Tl mining districts in Yunnan and Guizhou Provinces, respectively, in China, with those of surface and spring waters outside these mining districts.

Unfortunately, relatively little is known about the rates at which As is released to surface and ground waters during oxidation of As-bearing minerals, especially arsenopyrite, or the factors that determine whether the As will be released directly as As(III) or converted to As(V). Using  $\text{FeCl}_3$  as the oxidant, Rimstidt et al. (1994) studied the behaviour of arsenopyrite in acidic solutions, and proposed an equation to predict oxidation rates and associated activation energies for temperatures from 0 to 60 °C. However, they did not determine the valence state of the As in the solutions. Ehrlich (1964) investigated the bacterial oxidation of arsenopyrite in water, and concluded that the As is converted to As(V) but did not quantitatively evaluate the valence state of the As in the water. Finally, Maurizio et al. (1999) studied the mechanisms of arsenite oxidation in aqueous solution, using  $\text{H}_2\text{O}_2$  as an oxidant, and suggested that the rates of the oxidation of As(III) with  $\text{H}_2\text{O}_2$ , measured in NaCl solution varied as a function of pH (7.5–10.3), temperature and ionic strength ( $I=0.01\text{--}4$ ).

In addition to these experimental studies, there have also been a number of theoretical studies of the behaviour of As in surface and ground waters. For example, Levy et al. (1999) used the geochemical computer code PHREEQC to model the distribution of As in groundwaters in the eastern Owen Lake area of California, USA, and predicted that the distribution of As species is related to the redox state.

In this paper, the authors report the results of a kinetic experiment in a mixed flow reactor designed to investigate the aqueous oxidation of arsenopyrite and determine some of the factors controlling the concentration and valence state of As released to the solution when  $\text{Fe}_2(\text{SO}_4)_3$  is the oxidant. The study sheds new light on the potential effects to the environment of the exploitation of arsenopyrite ores, and provides a

theoretical basis for formulation of effective policies for the management of acidic mine waste water contaminated by As.

## 2. Experimental methods

### 2.1. Sample preparation

Experiments were conducted on arsenopyrite extracted from a quartz-sulphide vein located in the Jinjing mine, Tianzhu district in Guizhou Province, China. The composition of the arsenopyrite, based on electron microprobe analyses, is As (45.40%), Fe (34.93%) and S (19.45%) (average of 10 analyses). In addition, trace quantities of Au, Ag, Bi, Sn, Ca, Cu and Mn are present. Samples of the vein were crushed and ground to a grain-size of 60–80 mesh and hand-picked under the microscope to yield a concentrate containing ~99 vol.% arsenopyrite. The arsenopyrite was then washed in alcohol for 10 min, ultrasonically cleaned 3 times for 1 min to remove fine silty grains coated on the surface of crystals, washed with distilled water 3 times, washed with acetone twice, dried, and stored in a desiccator. Sixty grams of arsenopyrite were prepared in this manner. The amount of arsenopyrite and flow rate of the solution were varied in each experiment to accommodate the different rates of oxidation of arsenopyrite at the different temperatures and the oxidant concentration. In most experiments, the mass of arsenopyrite was around 0.7–0.9 g and the flow rate was 5–9  $\text{g min}^{-1}$ . This ensured that the concentration of As in the effluent was high enough to be measured accurately and that an experiment could be completed in a day.

The specific surface area of two samples of the unreacted arsenopyrite were measured to be 0.033  $\text{m}^2 \text{g}^{-1}$  and 0.031  $\text{m}^2 \text{g}^{-1}$  respectively, using a Quantachrome NOVA 1000 BET specific surface area and aperture distribution analyzer. The mean specific surface area of 0.032  $\text{m}^2 \text{g}^{-1}$  was employed in calculations of reaction rates.

Berner (1970) reported that dissolved Fe concentrations in acidic mine drainage waters are often as high as  $2\text{--}9 \times 10^{-3} \text{ mol kg}^{-1}$  and the pH value less than 2. In the

Table 1  
Selected solutes in water from the Nanhua–Lanmuchang area

Metal	As	Fe	$\text{Cl}^-$	$\text{SO}_4^{2-}$	Reference source
Mine water at As–Tl mining site	31 460	140	3380	1026.04	Zhong et al. (1997)
Spring water	2060	120	4250	5.35	Zhong et al. (1997)
Mining water at Hg–As–Tl mining site	14 903.7	177 894	11 310 <sup>a</sup>	274 110 <sup>a</sup>	Xiao et al. (1999)
Surface water	10.98	394	1190 <sup>a</sup>	3840 <sup>a</sup>	Xiao et al. (1999)

Unit:  $\mu\text{g l}^{-1}$ .

<sup>a</sup> Zhong et al. (1997).

present experiments, initial Fe(III) concentrations ranged from  $10^{-2}$  to  $10^{-5}$  mol  $\text{kg}^{-1}$  in order to understand the relationship between the rate of oxidation of arsenopyrite and the concentration of oxidant. All the solutions were prepared with deionized water, with  $\text{Fe}_2(\text{SO}_4)_3$  as the oxidant. Various concentration of  $\text{Fe}_2(\text{SO}_4)_3$  were prepared by diluting a  $0.4$  mol  $\text{kg}^{-1}$   $\text{Fe}_2(\text{SO}_4)_3$  solution, which was prepared by  $\text{H}_2\text{O}_2$  oxidation of  $\text{FeSO}_4 \cdot 7\text{H}_2\text{O}$  (analytical grade reagent). The concentrations of total Fe and  $\text{Fe}^{3+}$  were determined by potassium dichromate titration (Kolthoff and Stenger, 1942). The initial pH of the solution was adjusted to a value of 1.8 by adding a small amount  $\text{H}_2\text{SO}_4$ . Finally,  $\text{N}_2$  gas was bubbled through the solution in order to stir solutions and remove any dissolved  $\text{O}_2$ .

## 2.2. Experimental apparatus

The experiments were conducted using a pneumatically mixed flow reactor. This approach facilitated determination of reaction rates, as these can be determined directly from analyses of the effluent composition once the system has reached a steady state. The mixed flow reactor used in this study was designed and developed at the Institute of Geochemistry at the Chinese Academy of Sciences (Guiyang), and comprises a continuously stirred reactor equipped with a side arm (Fig. 1).

The reactor is made of GG-17 silica-borate glass (similar in composition to Pyrex), and consists of a main

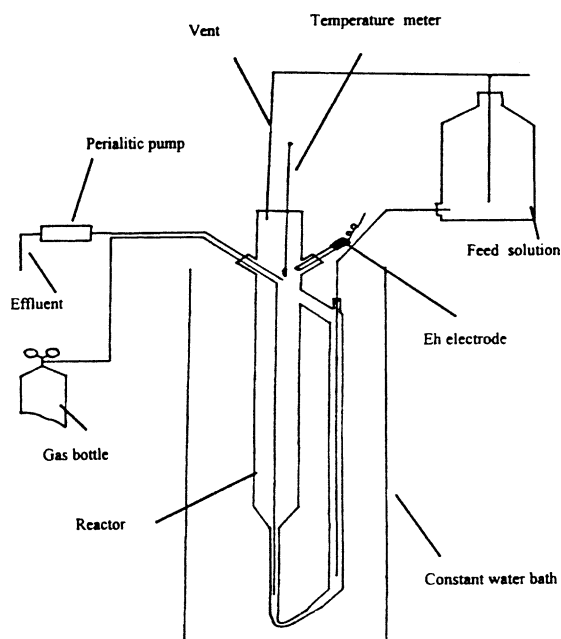


Fig. 1. Schematic drawing of the mixed flow reactor used in the experiments.

tube with an inner diameter of 5 cm (a height to diameter aspect ratio of 8) and a side arm with an inner diameter of 2 cm. The effective capacity of the reactor is 800 ml. During experiments,  $\text{N}_2$  gas was bubbled up from the bottom of the reactor and the solution was strongly stirred. This enabled suspension of the arsenopyrite grains thereby ensuring maximal contact with the flowing solution. Flow of solution through the reactor was achieved by supplying fresh solution using a Mariot constant-level bottle, and removing the reacted solution with a peristaltic pump. As long as the constant-level bottle is adjusted to the appropriate height, the solution-supply rate will be automatically adjusted according to the level of the upper surface of the solution in the reactor. After several minutes of operation, the in-flow and out-flow rates of the solutions concentration reached a constant value. The stability of the reactor was tested by passing a  $0.5$  mol  $\text{kg}^{-1}$   $\text{NaHCO}_3$  solution through it at a flow rate of  $10$  g  $\text{min}^{-1}$  and analysing the effluent. As can be seen from Fig. 2, the effluent reached a steady state concentration of  $0.5$  mol  $\text{kg}^{-1}$  after 80 min, which was maintained for the duration of the experiment (200 min). This indicated near perfect mixing of the tracer ( $\text{NaHCO}_3$ ) with the water.

During experiments, the reactor was immersed in a constant temperature bath, which maintained the temperature at a value that varied by  $\pm 0.05$  °C. The experiments were conducted at atmospheric pressure. Nitrogen gas was introduced at a rate of  $0.5$  l  $\text{min}^{-1}$  during experiments, which was sufficient to maintain the arsenopyrite grains in suspension and replace dissolved  $\text{O}_2$  so that the effects of Fe(III) as an oxidant could be measured directly. The progress of the reaction was monitored by measuring the redox potential of the solution using a 501 ORP combination pt/saturated KCl/Ag–AgCl electrode supplied by the Lei-Ci instrument company in Shanghai.

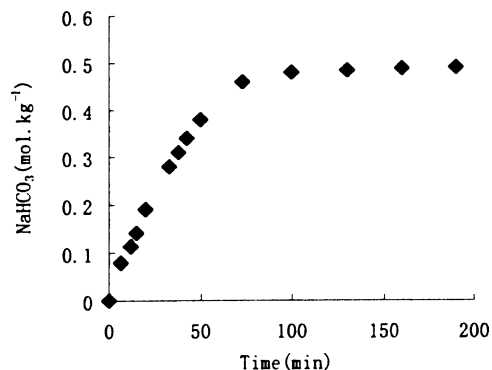


Fig. 2. Concentration–time graph for a  $\text{NaHCO}_3$  spike solution flowing through the mixed flow reactor at a rate of  $10$  g/min. The graph indicates that a steady state concentration is reached after 80 min.

### 2.3. Experimental procedure

Experiments were conducted at temperatures of 15, 25, 35 and 45 °C. The flow rate ranged from 5 to 9 g min<sup>-1</sup>. The duration of experiments varied between 6 and 8 h. At the start of each experiment, the feed solution was introduced into the reactor from the constant-level bottle. The reactor was then placed in a constant temperature bath and the flow of solution and N<sub>2</sub> gas was initiated. When the temperature in the reactor reached the required value and the redox potential remained constant, the experiment was started by adding a pre-determined amount of arsenopyrite to the reactor. For the initial experiments, a 50 ml fluid sample was collected and filtered every 5 min until the end of the experiment. The Eh of the solution in the reactor was recorded immediately after sampling. The sample solution was analysed for As, total Fe and Fe<sup>2+</sup>. After several experiments had been completed, it was found that Eh varied inversely with the concentration of As in the effluent. As is evident from Fig. 3, Eh decreased sharply with the addition of arsenopyrite at the start of an experiment (due probably to dissolution of finer particles) and then more slowly, while the concentration of As increased slowly and then gradually more rapidly. With continued oxidation, Eh eventually reached a steady state value and As a steady state concentration soon after. By monitoring the evolution of Eh values it was therefore possible to determine when As concentration had reached a steady state value. In subsequent experiments, the authors continued to measure Eh every 5 min but only sampled the fluid after Eh had maintained a steady state value for at least an hour. After completion of an experiment, the mineral grains were washed with distilled water and acetone, dried, and then stored in a desiccator.

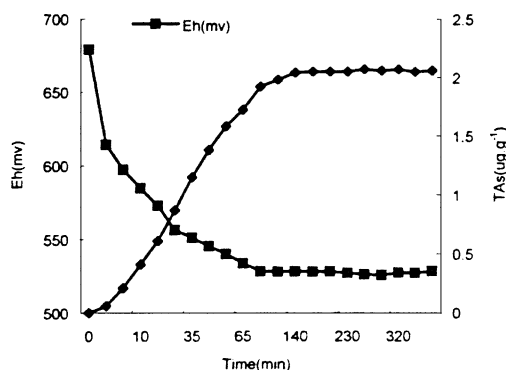


Fig. 3. Evolution of total As and Eh during oxidation of arsenopyrite.

### 2.4. Analytical method

The effluent solution was analysed for Fe and As and their valence states. Concentrations of Fe<sup>2+</sup> and total Fe (TFe) were determined spectrophotometrically in a 1,10-phenanthroline medium (Marczenko, 1976). The concentration of As and its valence state were determined using a modified molybdenum blue spectrophotometric method. In this method, As(V) in the sample is reacted with ammonium molybdate solution to produce heteropoly molybdarsenate (Onishi, 1986) which is then reduced with ascorbic acid (the valence of Mo is reduced), to form a blue coloured complex “molybdenum blue”. The concentration of this complex and, in turn, that of the arsenate [As(V)] is determined spectrophotometrically. This was done by placing the treated sample in a 1 cm cuvette and measuring the absorbance at a wavelength of 850 nm (wavelength of maximum absorbance for molybdenum blue) using a Shimadzu UV-VIS-3000 spectrophotometer. The concentration of As(V) was calculated by comparing the absorbance to that of a calibration curve for a set of standard As(V) solutions treated in the same way as the effluent solution except for acidification. The total As in the sample solution was determined by oxidizing the arsenite [As(III)] (which does not take part in the above reactions) to As(V) as follows: 1–2 drops of 1% potassium permanganate solution are added to the sample and a few minutes later, ammonium ferrous sulfate solution is added to remove excess oxidant. The rest of the procedure is the same as that described above. The concentration of As(III) in the effluent was calculated by subtracting the concentration of As(V) determined initially from that determined after oxidation of As(III). This method permits As to be analysed to a lower detection limit of 0.05 µg ml<sup>-1</sup>. Before and after each run, the arsenopyrite was examined with XPS using a PHI-5300ESCA instrument, in order to evaluate the valence state on the surface of grains.

## 3. Results and discussion

### 3.1. Data processing

As the experiment was carried out in a mixed flow reactor, the rate of oxidation of the arsenopyrite could be calculated directly using the relationship (Sheng et al., 1997)

$$r = (C_X - C_0)V/A \quad (1)$$

where  $r$  is the reaction rate (mol m<sup>-2</sup> s<sup>-1</sup>),  $C_X$  is the steady state concentration of an element in the effluent solution,  $C_0$  is the concentration of this element in the feed solution (mol kg<sup>-1</sup>),  $V$  is the mass flow rate (kg s<sup>-1</sup>), and  $A$  is the area of mineral surface exposed to the

solution ( $\text{m}^2$ ). The elements released when arsenopyrite is oxidized are primarily As, Fe(II) and S. As  $\text{Fe}_2(\text{SO}_4)_3$  was the active component in the solution used to oxidize arsenopyrite, only As could be used to determine the rate of reaction. Any minor amounts of As that have been introduced in preparing the oxidising solution were subtracted as the term  $C_0$ . The specific surface area of the arsenopyrite concentration was  $0.032 \text{ m}^2 \text{ g}^{-1}$ .

### 3.2. Influence of temperature and oxidant concentration on arsenopyrite oxidation

In order to evaluate the influence of temperature and oxidant concentration on As release during arsenopyrite decomposition, the As concentration have been plotted as a function of  $\log m_{\text{Fe}^{3+}}^+$  in Fig. 4, where the ordinate (TAs) represents the concentration of As released during oxidation of  $1 \text{ m}^2$  of arsenopyrite per minute. From this diagram it can be seen that the total As concentration (TAs) increases exponentially with increasing  $\text{Fe}_2(\text{SO}_4)_3$  concentration, especially at  $\text{Fe}_2(\text{SO}_4)_3$  concentrations higher than  $10^{-4} \text{ mol kg}^{-1}$ . It is also apparent that TAs increases sharply with increasing temperature. In other words oxidation of arsenopyrite and consequent release of As is very much dependent on the concentration of the oxidant and temperature.

The influence of Fe(III) concentration on the rate of oxidation of arsenopyrite can be evaluated using the following expression:

$$dn_{\text{Fe}^{3+}}^+/dt = r = k(m_{\text{Fe}^{3+}}^+)^n \quad (2)$$

where  $k$  is the reaction rate constant, and  $n$  is the reaction order for Fe(III). Taking the logarithm of both sides of Eq. (2), we obtain:

$$\log r = n \log m_{\text{Fe}^{3+}}^+ + \log k \quad (3)$$

as  $\log r$  and  $\log m_{\text{Fe}^{3+}}^+$  are linearly related, the influence of oxidant concentration on the rate of reaction can be quantified by plotting  $\log r$  [obtained from Eq. (1)]

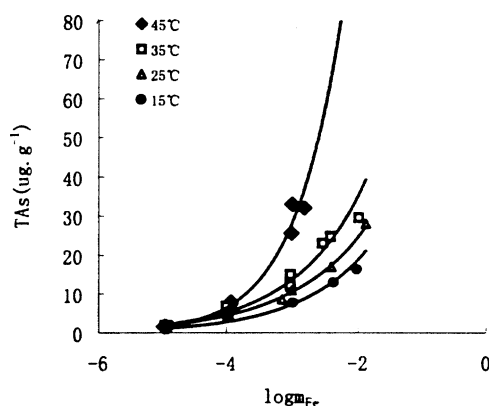


Fig. 4. Total As concentration in the effluent as a function of oxidant concentration ( $\log m_{\text{Fe}}$ ) and temperature.

against  $\log m_{\text{Fe}^{3+}}^+$ , and determining the reaction rate constant ( $\log k$ ) from the value of  $\log r$  at  $\log m_{\text{Fe}^{3+}}^+ = 0$  in a linear regression of the data.

In Fig. 5, the authors have plotted the reaction rates determined from the different experiments as a function of  $\log m_{\text{Fe}^{3+}}^+$  and separated the different data sets according to temperature (Table 2). As can be seen from Fig. 5 and Table 2, the rate of oxidation of arsenopyrite increases with increasing oxidant concentration and temperature. The reaction order is essentially constant with a value of 0.41 at temperatures from 15 to 35 °C but is significantly higher (0.64) for the experiments conducted at 45 °C. The corresponding changes in  $\log k$  are a small increase from  $-4.08$  to  $-3.77$  then a sharp decrease to  $-2.7$ , which implies a different reaction mechanism between 35 and 45 °C.

### 3.3. The valence state of As released during oxidation of arsenopyrite

As can be seen from Fig. 6, As released to the  $\text{Fe}_2(\text{SO}_4)_3$  solution during oxidation of arsenopyrite was mainly As(III), the proportion of As(V) was less than 20 mol%. However, concentration of As(III) took considerably longer to reach a steady state value than that of As(V), i.e., the proportion of As(V) relative to As(III) was significantly higher near the start of the reaction.

The authors believe that there are two sources of As(V) in the solutions, the one being already present on the surface of the arsenopyrite grains (presumably because of oxidation by air), which was preferentially transferred to the solutions near the start of the reaction, the other is from conversion of As(III) released to solution during the oxidation of arsenopyrite to As(V). In order to test these hypotheses, an additional set of experiments were conducted with a starting solution containing  $10 \text{ mg l}^{-1}$  As(III) and  $0.96 \times 10^{-3} \text{ mol kg}^{-1}$   $\text{Fe}_2(\text{SO}_4)_3$ . The results of these experiments are reported

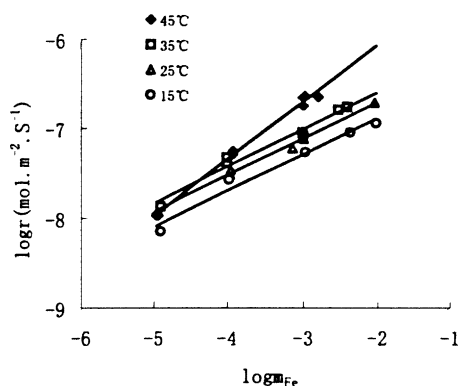


Fig. 5. The logarithm of the rate of oxidation of arsenopyrite ( $\log r$ ) as a function of oxidant concentration ( $\log m_{\text{Fe}}$ ) and temperature.

in Table 3 and illustrated in Fig. 7. As can be seen from this figure, As(III) was only slowly oxidised to As(V), confirming that the source of As(V) in the solution was mainly As(V) initially present on the surface of the arsenopyrite. This conclusion is also supported by the XPS analyses (Table 4). These XPS analyses revealed that, before reaction, As was present on the surface of

Table 2

Regression equations for some of the experimental results

<i>Fig. 4</i>		
45 °C	$Y = 5073.3 \times 10^{1.46x}$	$R^2 = 0.9952$
35 °C	$Y = 544.0 \times 10^{0.99x}$	$R^2 = 0.9785$
25 °C	$Y = 317.1 \times 10^{0.86x}$	$R^2 = 0.994$
15 °C	$Y = 295.0 \times 10^{0.96x}$	$R^2 = 0.9813$
<i>Fig. 5</i>		
45 °C	$Y = 0.641x - 2.7833$	$R^2 = 0.995$
35 °C	$Y = 0.414x - 3.7722$	$R^2 = 0.9768$
25 °C	$Y = 0.4084x - 3.8914$	$R^2 = 0.9874$
15 °C	$Y = 0.4049x - 4.0817$	$R^2 = 0.975$
<i>Fig. 10</i>		
35 °C (FeCl <sub>3</sub> )	$Y = 8193.8 \times 10^{1.92x}$	$R^2 = 0.98$
35 °C (Fe <sub>2</sub> (SO <sub>4</sub> ) <sub>3</sub> )	$Y = 611.0 \times 10^{0.97x}$	$R^2 = 0.96$

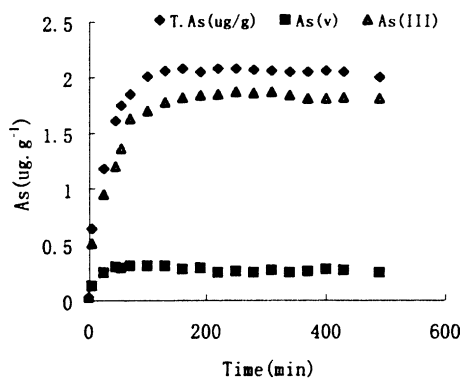


Fig. 6. The distribution of As species in the effluent during oxidation of arsenopyrite at 35 °C; pH = 1.8,  $m_{\text{Fe}_2(\text{SO}_4)_3} = 0.98 \times 10^{-3} \text{ mol kg}^{-1}$ .

Table 3

The effect of anion species on oxidation of  $[\text{TAs-As(V)}]/\text{TAs}$  (%)

Time (h)	FeCl <sub>3</sub>	Fe <sub>2</sub> (SO <sub>4</sub> ) <sub>3</sub>
0	92	99
1	76	98
2	5	97
3	2	94
5.45	0.8	94
7.15	0.4	93

the arsenopyrite grains as As(V), whereas after reaction with a solution having a Fe<sub>2</sub>(SO<sub>4</sub>)<sub>3</sub> concentration of  $1 \times 10^{-4} \text{ mol kg}^{-1}$ , the As on the surface of arsenopyrite grains was present as As(III), indicating As(V) initially present on the surface of the arsenopyrite was dissolved. As for the conversion of As(III) to As(V), either it occurred in solution or on the surface of arsenopyrite grains and was then released to the solution. Additional experiments are needed to distinguish between these two phenomena.

Table 5 and Fig. 8 indicate that the proportion of As(III) increased with increasing temperature and decreased with increasing concentration of the oxidant Fe<sub>2</sub>(SO<sub>4</sub>)<sub>3</sub>, especially at 15 and 25 °C.

The extent of oxidation of As(III) to As(V) varied significantly with oxidant concentration and temperature. At temperatures up to and including 35 °C, the proportion of As(V) increased with increasing oxidant concentration (Fig. 8). However, in the experiments at 45 °C this trend was reversed and even in the experiments conducted at 35 °C the rate of increase in the proportion of As(V) with increasing oxidant concentration was lower than in the experiments at 15 and 25 °C. At the lowest oxidant concentrations employed, the proportion of As(V) was highest in the experiment at 45 °C and lowest in the experiment conducted at 25 °C, whereas at the highest oxidant concentrations, the proportion of As(V) decreased systematically with increasing temperature. The behaviour of As in high temperature solutions (Fig. 8) may be related to the fact that the experiments were conducted in a flow reactor, i.e., the reactor was continuously fed with a solution having a constant composition of Fe<sub>2</sub>(SO<sub>4</sub>)<sub>3</sub> concentration. The rate of production of As(III), as discussed earlier, was highest when the oxidant concentration and temperature were highest, thus, the rate of consumption of oxidant in producing As(III) greatly exceeded the rate

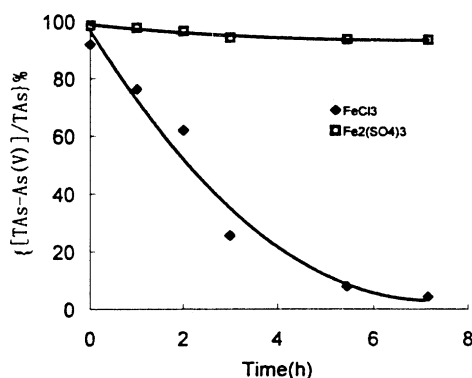


Fig. 7. Evolution of As(III) concentration at 35 °C as a function of oxidant type, i.e., Fe<sub>2</sub>(SO<sub>4</sub>)<sub>3</sub> versus FeCl<sub>3</sub>; in the experiments with FeCl<sub>3</sub> as the oxidant,  $m_{\text{FeCl}_3} = 0.907 \times 10^{-3} \text{ mol kg}^{-1}$ , and  $\text{TAs} = 3.57 \text{ mg l}^{-1}$  in those with Fe<sub>2</sub>(SO<sub>4</sub>)<sub>3</sub> as the oxidant,  $m_{\text{Fe}_2(\text{SO}_4)_3} = 0.96 \times 10^{-3} \text{ mol kg}^{-1}$ , and  $\text{TAs} = 3.43 \text{ mg l}^{-1}$ .

of supply in such experiments, thereby minimizing the amount that was available to convert the As(III) to As(V), that is, As(V) decreases with increasing temperature and oxidant concentration, whereas in the lower temperature experiments, the reaction rates were much lower, leaving more oxidant to convert As(III) to As(V). In order to confirm the above hypothesis the standard As(III) solution was reacted with  $10^{-3}$  mol  $\text{kg}^{-1}$   $\text{Fe}_2(\text{SO}_4)_3$  solution at the same temperatures employed in the experiments. As is evident from Fig. 9, the proportion of As(V) actually increases with increasing temperature, which implies that it is unsuitable to study valance change of an element using this flow reactor.

It is concluded that when arsenopyrite is oxidised in a  $\text{Fe}_2(\text{SO}_4)_3$  solution, at the start of an experiment As(V) is already on the surface of the arsenopyrite and is preferentially transferred to the solution. Subsequently, As(III) is first released and then converted to As(V) at a

rate that increases with increasing concentration of oxidant and temperature.

### 3.4. The influence of anionic species on the oxidation of arsenopyrite and As(III)

In order to obtain information on the effect of the anionic component of the oxidant, arsenopyrite was reacted with a  $\text{FeCl}_3$  solution at 35 °C and, as was the case for  $\text{Fe}_2(\text{SO}_4)_3$ , also a standard As(III) solution was reacted with this oxidant. The results of these two experiments are shown in Table 6 and Figs. 10 and 7, respectively. The results of these experiments indicate that the rate of oxidation of arsenopyrite with  $\text{FeCl}_3$  is far higher than with  $\text{Fe}_2(\text{SO}_4)_3$ , especially for high concentrations of the oxidant (Fig. 10). The concentration of As dissolved with  $\text{FeCl}_3$  as the oxidant is about 5 times that with  $\text{Fe}_2(\text{SO}_4)_3$  (Table 6) at  $\log m_{\text{Fe}^{3+}} = -1.99$ . The rate of oxidation of As(III) with  $\text{FeCl}_3$  as the oxidant was

Table 4  
The xps analyses of arsenopyrite surface before and after reaction

Sample	Etched depth (nm)	Element	Atomic ratio (S=1)	Valence state
Arsenopyrite before reaction	0.0	C		
		O	15.6	-2
		S	1	+6
		Fe	1.43	+3
		As	1.87	+5
Arsenopyrite after reaction	0.0	C		
		O	6.9	-2
		S	1	-1, +6
		Fe	0.78	+3
		As	0.98	+3

Table 5  
Data of oxidation of arsenopyrite used in Figs. 5 and 8

$\text{Log} m_{\text{Fe}}$	$\text{Log } r$	[As(III)/TAs] (%)	$\text{Log } m_{\text{Fe}}$	$\text{Log } r$	[As(III)/TAs] (%)
45 °C			35 °C		
-2.8	-6.65		-4	-7.38	85.71
-3	-6.75	93.24	-3.01	-7.05	80.34
-2.88	-6.64	95.08	-3	-7.09	
-3	-6.66		-2.41	-6.76	76.82
-4.96	-7.97	59	-4	-7.33	
-3.92	-7.26	78.21	-2.41	-6.77	
-4.95	-7.95		-2.53	-6.80	
-4.93	-7.97				
25 °C			15 °C		
-3.96	-7.52	89.39	-2.02	-6.94	40.94
-3.95	-7.47	91.48	-2.37	-7.05	52.92
-3.14	-7.23	79.45	-4.90	-8.15	91.30
-2.99	-7.12	71.67	-2.97	-7.27	63.23
-2.04	-6.71	53.25	-3.97	-7.57	72.71
-3	-7.09				

also higher than with  $\text{Fe}_2(\text{SO}_4)_3$ . After 7 h, 96% of the As(III) had been oxidised when  $\text{FeCl}_3$  was the oxidant, whereas in the  $\text{Fe}_2(\text{SO}_4)_3$  solution only 6.7% of As(III) had been oxidized after the same period of time, i.e., oxidation was 16 times faster with  $\text{FeCl}_3$ . Thus, although arsenopyrite will oxidize more rapidly in the presence of acidic solutions with high concentrations of  $\text{Cl}^-$  than those with high concentrations of  $\text{SO}_4^{2-}$ , the resulting impact on the environment will be lower. This is because As(III) is 60 times more acutely toxic than As(V) and a much higher proportion of As(III) is converted to As(V) with  $\text{FeCl}_3$  than with  $\text{Fe}_2(\text{SO}_4)_3$  (16 times in the above experiments).

Using the chemical equilibrium model MINTQA2 and the concentration of  $\text{Fe}^{3+}$  used in this study to model the main distribution of  $\text{Fe}^{3+}$  species in the  $\text{FeCl}_3$  and  $\text{Fe}_2(\text{SO}_4)_3$  solutions, respectively, it was found that there are large differences in the main distribution of  $\text{Fe}^{3+}$  species between these two solutions. Compared with the  $\text{Fe}_2(\text{SO}_4)_3$  solutions,  $\text{Fe}^{3+}$ ,  $\text{FeOH}^{2+}$  and  $\text{FeCl}^{2+}$  are greater in the  $\text{FeCl}_3$  solutions. For example, At 25 °C the distribution of species is  $\text{Fe}^{3+}$  (66.4%),  $\text{FeOH}^{2+}$  (14.1%) and  $\text{FeCl}^{2+}$  (16.3%) in the  $\text{FeCl}_3$  solutions, compared to only  $\text{Fe}^{3+}$  (7.4%),  $\text{FeOH}^{2+}$  (1.4%) and  $\text{FeSO}_4^+$  (84.7%) in the  $\text{Fe}_2(\text{SO}_4)_3$  solutions. These results suggest a greater oxidation

capacity in a  $\text{FeCl}_3$  solution compared to a the  $\text{Fe}(\text{SO}_4)_3$  solution because the activity of Fe(III) is much higher with the  $\text{FeCl}_3$  solutions and both of  $\text{FeOH}^{2+}$  and  $\text{FeCl}^{2+}$  are photochemically active. According to Hug (2001) and Emett and Khoe (2001), in acidic solutions ( $\text{pH} < 5$ ),  $\text{FeOH}^{2+}$  and  $\text{FeCl}^{2+}$  will absorb photons and produce hydroxyl radicals ( $\cdot\text{OH}$ ) and dichloro radicals ( $\cdot\text{Cl}_2$ ) which are very strong oxidants. In contrast,  $(\text{FeSO}_4)^+$  does not produce free radicals when illuminated by ultraviolet light. Obviously, the capability of  $\text{FeCl}_3$  to oxidize arsenopyrite and As(III) must be greater than that of  $\text{Fe}_2(\text{SO}_4)_3$  even though this experiment was done under sunlight.

The authors therefore believe that the main reason causing the difference in the capability of oxidizing arsenopyrite and As(III) is the nature of this two solutions, the affinity of Fe(III) and  $\text{SO}_4^{2-}$  is more stronger than that of Fe(III) and  $\text{Cl}^-$ , which produces more Fe(III) ion and its hydroxide and chloride complexes in  $\text{FeCl}_3$  solutions.

### 3.5. Implications for arsenopyrite oxidation in the natural environment

The results of this study indicate that in the presence of solutions with high concentrations of  $\text{Fe}_2(\text{SO}_4)_3$

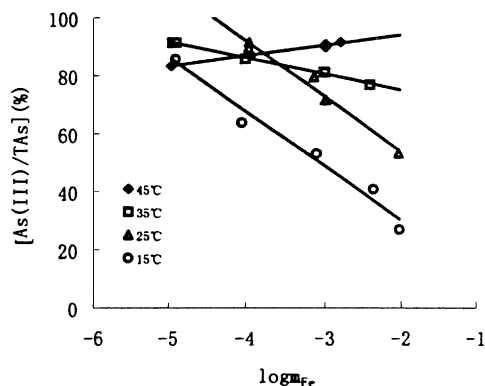


Fig. 8. Oxidation of As(III) as a function of oxidant concentration ( $\log m_{\text{Fe}}$ ) and temperature.

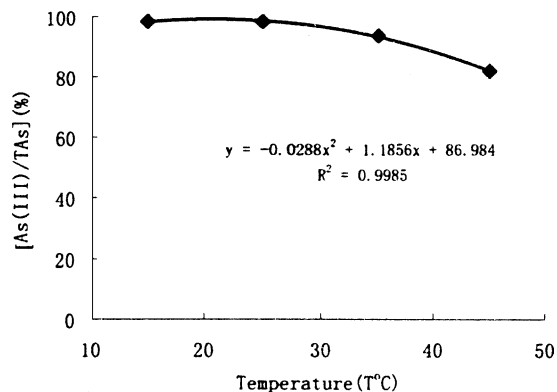


Fig. 9. The influence of temperature on As(III) oxidation.

Table 6  
The effect of anion species on oxidation of arsenopyrite

$\text{Fe}_2(\text{SO}_4)_3$ ( $\log m_{\text{Fe}}$ )	TAs ( $\mu\text{g g}^{-1}$ )	$\text{FeCl}_3$ ( $\log m_{\text{Fe}}$ )	TAs ( $\mu\text{g g}^{-1}$ )
-1.99	29.56	-2.02	171.4
-2.41	24.81	-2.48	100.46
-2.41	24.65	-4	8.55
-2.53	22.96	-3.99	6.02
-3	23	-4.97	2.02
-3.99	8.03	-2.63	45.44
-4.90	1.93	-3	43.55
-4.94	1.85	-3.99	8.63



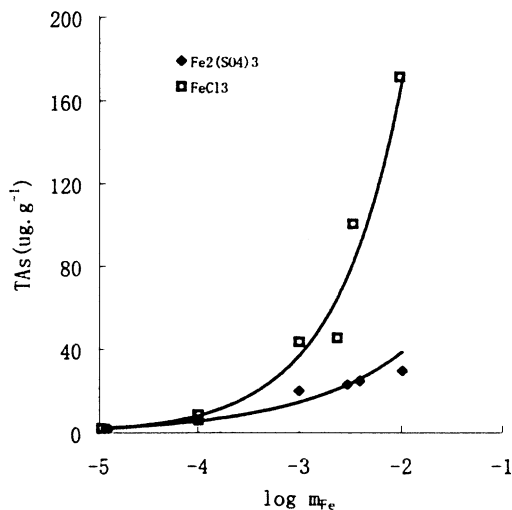


Fig. 10. The influence of oxidant type, i.e.,  $\text{Fe}_2(\text{SO}_4)_3$  versus  $\text{FeCl}_3$ , on arsenopyrite at 35 °C.

(produced in nature by the interaction of meteoric waters with pyrite) arsenopyrite breaks down rapidly releasing As. This result is confirmed in some areas. For example, in underground and surface waters from the Lanmuchang Hg–As–Tl mining district in Guizhou Province, China, Zhang et al. (1997) reported that the concentration of  $\text{SO}_4^{2-}$  and  $\text{Cl}^-$  was  $2.8 \times 10^{-3} \text{ mol kg}^{-1}$  and  $3.1 \times 10^{-4} \text{ mol kg}^{-1}$ , respectively. Xiao et al. (1999) reported concentrations of As of up to  $14.90 \text{ mg l}^{-1}$ , which is 298 times more than the maximum acceptable As concentration in drinking water ( $0.05 \text{ mg l}^{-1}$ ) recommended by the World Health Organization. From Fig. 10, it can be seen that the contribution of the concentration of  $\text{Cl}^-$  to the As pollution in Lanmuchang Hg–As–Tl mining district was less than  $\text{SO}_4^{2-}$ , i.e., the effect of released As on the health of local people at the initial stages of the oxidation of arsenopyrite in this area may be serious because more As(III) is present in underground and surface waters.

It is concluded that oxidation of arsenopyrite exposed naturally at the surface or by mining activity is the principal factor responsible for the pollution of groundwaters by As(III) in areas known to be underlain by rocks containing arsenopyrite-bearing mineral deposits and that such pollution occurs extremely rapidly.

#### 4. Conclusions

(1) In acidic solutions ( $\text{pH} = 1.8$ ,  $M_{\text{Fe}_2(\text{SO}_4)_3} = 10^{-2}$  to  $10^{-4}$ ) the rates of oxidation of arsenopyrite increase with increasing oxidant concentration and reaction temperature;

(2) Arsenic released during oxidation of arsenopyrite is present dominantly as aqueous As(III). Arsenic(V) is present in subordinate concentrations, and is mostly derived from the preoxidized outermost layer of the sample used in the experiments. In  $\text{Fe}_2(\text{SO}_4)_3$  solutions, the oxidation of As(III) to As(V) proceeds very slowly so that As(III) persists in the solution. The conversion rate of As(III) to As(V) tends to increase with increasing oxidant concentration and reaction temperature.

(3) The rate of oxidation of arsenopyrite with  $\text{FeCl}_3$  as the oxidant is considerably higher than that with  $\text{Fe}_2(\text{SO}_4)_3$ , especially for high oxidant concentration.

(4) Exploitation of arsenopyrite-bearing sulfide ores in mining districts is a major health hazard because oxidation of arsenopyrite by acidic water is extremely rapid and the As is released as the more toxic As(III) form.

#### Acknowledgements

This study is part of a CIDA-sponsored Sino-Canadian Cooperation Program (CIDA). The authors wish to thank Professor C. Gammons for his help with the design of this research project. The research was supported financially by the National Natural Science Foundation of China (Grant No. 49773202) and the Open Laboratory of Ore Deposit Geochemistry, Institute of Geochemistry, Chinese Academy of Sciences. Professor Zeng Yishan provided us with samples arsenopyrite for use in the experiments, Professor Wang Fuya determined the surface area of the arsenopyrite charges, and Professor Ye Chuanxian analyzed the concentrations of Fe and As in the solutions. We also would like to thank Regina Tempel and Donald Rimstidt for the helpful review comments.

#### References

- Berner, R.A., 1970. Low temperature geochemistry of iron. In: Wedepohl, K.H. (Ed.), Handbook of Geochemistry. Springer Verlag, Berlin (Section 26, II-3).
- Bottomley, D.J., 1984. Origins of some arseniferous groundwater in Nova Scotia and New Brunswick. Can. J. Hydrol 69, 223–257.
- Ehrlich, H.L., 1964. Bacterial oxidation of arsenopyrite and enargite. Econ. Geol. 59, 1306–1312.
- Emett, M.T., Khoe, G.H., 2001. Photochemical oxidation of arsenic by oxygen and iron in acidic solutions. Water Res. 35, 649–656.
- Lixian, H., Ruolan, Z., Liqing, L., 1993. The geology of gold ore deposits in Guizhou. Geological Publishing House, pp. 54–73 (in Chinese).
- Onishi, H., 1986. Photometric Determination of Trace of Metals. John Wiley and Sons (Part IIA, p. 146).

- Hug, S.J., 2001. An adapted water treatment option in Bangladesh: solar oxidation and removal of arsenic (SORAS). *Environ. Sci.* 8, 467–479.
- Levy, D.B., Schramke, J.A., Esposito, K.J., Erichson, T.A., Moore, J.C., 1999. The shallow ground water chemistry of arsenic, fluorine and major elements: Eastern Owens Lake, California. *Appl. Geochem.* 14, 53–65.
- Kolthoff, I.M., Stenger, V.A., 1942. *Volumetric Analysis*, Vol. 3, 2nd Edition. Interscience Publishers, New York.
- Marczenko, Z., 1976. *Spectrophotometric Determination of Elements*. John Wiley and Sons, New York.
- Maurizio, P., Luigi, C., Frank, J.M., 1999. Arsenite oxidation by  $H_2O_2$  in aqueous solutions. *Geochim. Cosmochim. Acta* 63, 2727–2735.
- Rimstidt, J.D., Chermak, J.A., Gagen, P.M., 1994. Rates of reaction of galena, sphalerite, chalcopyrite and arsenopyrite with Fe(III) in acidic solutions. In: Alpers, C.N., Blowes, D.W. (Eds.), *Environmental Geochemistry of Sulfide Oxidation*. ACS Symp. Series 550. American Chemical Society, pp. 2–13.
- Sheng, Z., Tongjing, L., Liankui, W., 1997. The principle of geochemically dynamic reactor and the equation of velocity determination. *Geology-Geochemistry* 1, 53–58 (in Chinese).
- Xiao, T., Boyle, D., Guha, J., Hong, Y., Zheng, B., 1999. Hydrogeochemistry of toxic metals in a Au-As-Hg-Tl mineralized area in southwestern Guizhou, China. *Chinese Sci. Bull.* 44 (Suppl. 2), 171–172.
- Zhong, Z., Baogui, Z., Jiangbing, L., 1997. Research on environmental pollution of thallium during mining of thallium ore deposit in China. *Science in China (series D)* 27 (4), 331–336 (in Chinese).